Nanohybrids of Magnetic Iron-Oxide Particles in Hydrophobic Organoclays for Oil Recovery

Ru-Siou Hsu,[†] Wen-Hsin Chang,[†] and Jiang-Jen Lin*[,†,‡]

Institute of Polymer Science and Engineering, National Taiwan University, Taipei, Taiwan, and Department of Materials Science and Engineering, National Chung Hsing University, Taichung, Taiwan

ABSTRACT Nanohybrids with magnetic iron-oxide nanoparticles (FeNPs) embedded in the multilayered silicate clay were synthesized by in situ Fe^{2+}/Fe^{3+} coprecipitation. The natural clay, sodium montmorillonite (Na^+-MMT), was first modified with hydrophobic poly(oxypropylene)amine salts (POP at 2000 and 4000 g/mol M_w). The two POP-intercalated organoclays, with a silicate interlayer expansion from 1.2 to 5.2 and 9.2 nm, respectively, are suitable for embedding FeNPs. The presence of POP organics in layered structure created the space for intercalating with FeNPs of 2−4 nm in diameter, observed by transmission electronic microscope. The synthesized nanohybrids of POP4000/MMT-FeNP was composed of 17% iron oxide and 51 wt % POP within the silicate basal spacing of 5.0 nm. In contrast, the lower molecular weight of POP2000 intercalated MMT failed to encapsulate FeNPs in a significant amount, but resulting a "crowding-out effect" that caused the silicate interlayer space to shrink from 5.2 to 1.8 nm because of the replacement of the POP salt by Fe^{2+}/Fe^{3+} ions. The synthesis required the use of high molecular weight POP4000 and low temperatures (<4 °C) for a better dispersion in the reaction medium. The presence of POP in the layered silicate facilitated a homogeneous POP/MMT in water, associating with Fe^{2+}/Fe^{3+} ions and spatially accommodating for the subsequently generated FeNPs. The synthesized nanostructure consisting of POP and FeNP could be used as a pollutant remedy because of its ability to adsorbing crude oil and it is maneuverable under an applied magnetism.

KEYWORDS: iron oxide • layered silicate • magnetic • clay • crude oil • pollution remedy.

INTRODUCTION

Magnetic iron-oxide nanoparticles (FeNPs) are well-known for their wide applications including drug delivery (1) and magnetic resonance imaging (MRI) (2) because of the biocompatibility and high-density for digital storage (3). Different synthetic methods including coprecipitation (4, 5), microemulsion (6), electrochemistry (7), pyrolysis (8), and hydrothermal synthesis (9) have been reported. One of the most convenient methods for the Fe_3O_4 synthesis is the coprecipitation of Fe^{2+}/Fe^{3+} salts under mild temperatures and pH control, as described in the following equation

$$2FeCl_3 + FeCl_2 + 8NH_3 + 4H_2O \rightarrow Fe_3O_4 + 8NH_4Cl$$

For incorporating iron-oxide particles in the silicate clay structures, Yamanaka et al. reported the uses of high surface MMT clay to adsorb the particles (10). Similar materials have been reported for industrial applications (11−15). It was proposed that the magnetic adsorbents could be used to remove metal contaminants in aqueous medium or gaseous effluents (16, 17). Booker et al. found that magnetic particles could accelerate the coagulation of sewage (18) and Orbell et al. applied polymer-coated magnetic particles for oil spill remediation (19). In addition, Oliveira et al. reported the complex of silicate clay and magnetic iron oxide (Fe_2O_3 or Fe_3O_4) for high-surface adsorbent (17). These studies indicate the potential applications for combining the magnetic iron oxide particles and high surface clays; however, these hybrid materials have been limited to hydrophilic silicate clays. The natural phyllosilicate clays of the 2:1 type including the common smectite MMT clay are conventionally utilized as catalysts (20−22), adsorbents (23, 24), metal chelating agents (25), and fillers for polymer composites (26−28). Smectic clays are abundant in nature and well-characterized for their lamellar structure, high surface area, and cationic charges (29−32). These layered silicates, hydrophilic and swelling in water, occur in nature as aggregates in stacks of about micrometer sizes consisting of multilayered plates of aluminum and silicate oxides. Counter metal ions originate from the isomorphic substitution of silicon or aluminum by divalent metal ions such as Mg^{2+}, Ca^{2+}, or Fe^{2+}. For the ionic exchange capability, the divalent counterions in most natural clays could be exchanged into different cationic species including Na^+, Cu^{2+}, Zn^{2+}, Mg^{2+}, Ca^{2+}, and acidified H^+ form (33). The potential for the replacing priority is $Al^{3+} > Ca^{2+} > Mg^{2+} > K^+ = NH_4^+ > Na^+$ (22, 34). According to this exchange trend, organic quaternary ammonium salts can intercalate into the layered structure through the exchange reaction with Na^+. Recent efforts on developing the polymer/layered silicate nanocomposites (35, 36) have advanced the technique of converting the clays from hydrophilic to hydrophobic by ionic exchange reaction with organic amine salts (29−31, 37, 38). The use of high-molecular-weight polyoxyalkyleneamine salts was

* Corresponding author. Tel.: +886-2-3366-5312. Fax: +886-2-8369-1384. E-mail: jianglin@ntu.edu.tw.

Received for review January 9, 2010 and accepted April 9, 2010

[†] National Taiwan University.

[‡] National Chung Hsing University.

DOI: 10.1021/am100019t

particularly effective for expanding their high layer spacing (39−41). In addition, the modified organoclays became compatible for polymers as well as biomaterials such as proteins (42, 43). Herein, we report for the first time the preparation of hydrophobic clays for encapsulating magnetic FeNPs. The multilayered structure of the natural MMT was modified by hydrophobic poly(oxypropylene)-amine salts (POP) of two different molecular weights and then incorporated with FeNPs by in situ Fe^{2+}/Fe^{3+} coprecipitation. The spatial layer spacing with the POP presence is essential for associating with the proper ratio of Fe^{2+}/Fe^{3+} species and subsequently the generated FeNPs. The ultimate coexistence of hydrophobic POP and magnetic FeNPs in the silicates results in nanohybrids able to adsorb oil, agglomerating into large lumps and still physically maneuverable by an applied magnetic field. The materials with both properties of hydrophobic adsorption and susceptibility to magnetic field are proposed to physically manipulate pollutants or materials such as in oil-spill recovery and drug delivery, respectively.

EXPERIMENTAL SECTION

Materials. Sodium montmorillonite (Na^+-MMT, cationic exchange capacity of 1.20 mequiv/g CEC) was supplied by Nanocor Inc. The generic structure is 2:1 type of layered smectite aluminosilicates (28), composed of two tetrahedron sheets sandwiching an edge-shared octahedral sheet with a dimension of approximately 100 × 100 × 1 nm^3 for individual plate, and 8−10 plates for an average primary stack (32). Counter metal ions populate the composition with variation in isomorphic substitution of silicon or aluminum by divalent metal ions such as Mg^{2+}, Ca^{2+}, or Fe^{2+}. These ionic charges are potentially exchangeable with alkali metal ions such as Na^+ or Li^+ as well as organic ions. These layered silicates are hydrophilic and swell in water, but often exist as aggregates of micrometer sizes. Analytical grade of iron(II) chloride tetrahydrate ($FeCl_2 \cdot 4H_2O$) and iron(III) chloride hexahydrate ($FeCl_3 \cdot 6H_2O$) were purchased from SHOWA Chemical Co., Ltd. Concentrated ammonium hydroxide (28−30 wt %) was purchased from J.T. Baker and diluted in deionized water to 0.7 M solution prior to use. Poly(oxypropylene)- (POP-) backboned diamines were purchased from Huntsman Chemical Co. The POP-diamines of 2000 and 4000 M_W (abbreviated as POP2000 and POP4000, respectively) were used in this study.

Intercalation of Montmorillonite with Poly(oxypropylene)-diamines. Na^+-MMT (10 g, 1.20 mequiv/g) was swollen in deionized water (800 mL) at 80 °C with a constant stirring for several hours. The intercalating agent was prepared by POP2000 (24 g, 12 mmol) and concentrated hydrochloric acid (37 wt %, 6.0 mmol, acidification ratio of $H^+/NH_2 = 1/2$) in water and then added in one portion into the Na^+-MMT slurry. The mixture was stirred vigorously by a mechanical stirrer at 80 °C for 5 h and cooled to room temperature. The precipitate was collected through a vacuum filter and washed with toluene for three times to remove free amines. The POP2000/MMT was dried in an oven at 70 °C for 12 h and ground into powder in a high speed grinder. POP4000/MMT was similarly prepared.

Incorporation of Iron Oxide with the Organoclays (Method A). The solution of 2.0 M Fe^{2+} was prepared by dissolving $FeCl_2 \cdot 4H_2O$ (1.99 g, 10.0 mmol) in HCl (5 mL of 2.0 M) and the solution of 1.0 M Fe^{3+} from $FeCl_3 \cdot 6H_2O$ (1.35 g, 5.00 mmol) in HCl (5 mL of 2.0 M). A mixture of the 2.0 M Fe^{2+} solution (0.2 mL) and 1.0 M Fe^{3+} solution (0.8 mL) was added to the dispersion of POP2000/MMT (0.43 g in 17 mL water) at 4 °C while stirring for 3 h. The mixed dispersion (POP2000/MMT-Fe^{2+}/Fe^{3+}) at 1:2 molar ratio of Fe^{2+}/Fe^{3+} was then added with NH_4OH (40 mL, 0.7 N) while stirred. The crude products were isolated by centrifuging, washed with deionized water three times, and air-dried at room temperature. The iron-oxide samples with the other clay supports were prepared at 4 °C using a similar procedure.

Preparation of Organoclay-Iron Oxide Hybrids (Method B). For the preparation of POP2000/MMT-iron-oxide hybrids at 5/1 of organoclay to iron-oxide weight ratio, the homogeneous POP2000/MMT dispersion (0.43 g in 17 mL of D.I. water at 4 °C) was adjusted to pH 2. A mixture of Fe^{2+} solution (0.20 mL of 2.0 M solution) and Fe^{3+} solution (0.80 mL of 1.0 M) was added to the dispersion and stirred vigorously at 4 °C for 3 h. The addition was followed by a portion of aqueous NH_4OH (40 mL, 0.70 N) until the dispersion reached a pH of about 9−10. The crude products were obtained by repetitively centrifuging and washing with deionized water for a total of three times and then air-dried at room temperature. Using similar procedures, the POP4000-derived hybrid was also prepared.

Oil Adsorption. The typical procedure for measuring the extent of oil-adsorption is described below. Experiments were done using a mechanical stirrer and optionally with ultrasonic vibration for mixing. The organoclay (0.50 g in powder form) was dispersed in water (20 g), brought to 0 °C,and then added to the crude oil sample (0.80 g) in one portion. After being stirred for 30 min, the ice bath was removed to allow the reaction to reach room temperature. During the process, the oil−clay slurry slowly aggregated into lumps and precipitated out from the clear water phase. The temperature was cycled between ice bath and ambient temperatures several times. An incremental amount of crude oil was added each time at the lower temperature until reaching a maximum adsorption. Both organoclays, POP2000/MMT and POP4000/MMT, were dispersible at the lower temperatures but formed aggregates at ambient temperature. For the oil adsorption onto the composite of organoclay-iron oxide, the composite (0.10 g) was dispersed in water (10 g) at room temperature and crude oil was added in incremental amounts until reaching a maximum adsorption.

Characterization. X-ray powder diffraction (XRD) was performed on a Rigaku D/DAX-IIB with a Cu target ($\lambda = 1.5418$ Å) at a generator voltage of 30 kV, and current of 20 mA to measure the basal spacing (d spacing) of intercalated silicate clays, iron oxide and the composites. The basal spacing ($n = 1$) was calculated according to Bragg's equation ($n\lambda = 2d\sin\theta$) through the observed peak of $n = 2$, 3, etc. The estimation is possible only when the pattern has more than two peaks. The magnetization of organoclay-iron oxide composites was measured by a superconducting quantum interference device magnetometer (SQUID, MPMS5) at 298 K and ±10 000 G applied magnetic field. Thermal gravimetric analysis (TGA) was measured by using a Perkin-Elmer Pyris 1 model at a heating rate of 10 °C/min up to 800 °C under air flow to determine the weight loss of organic fraction. Transmission electron microscope (TEM) was performed on a JEOL JEM-1230 TEM equipped with Gatan Dual Vision CCD Camera. The samples were prepared by curing with diglycidyl ether of bisphenol A and Jeffamine D400 and then trimmed with the Leica Ultracut UCT6 and an Element Six Drukker ultramicrotome knife at room temperature.

RESULTS AND DISCUSSION

Characterization of POP/MMT Organoclays and Their Low-Temperature Dispersion Property. The intercalation of fatty alkyl quaternary amine surfactants (44) and POP-backboned amine salts (45) into Na^+-MMT layered structure was previously described. A wide expansion of the silicate basal space as high as 9.2 nm has been achieved (46−53). The organic incorporation expands

Table 1. Basal Spacing and Organic Embedment of the POP-Amine Salts/MMT-Iron Oxide Composites

	weight ratio	*d* spacing (Å)	organic fraction (wt %)[a]	crowding-out effect (%)[b]	magnetism (emu/g)	ability of crude oil adsorption[c]
Na^+-MMT		12	0			<1
POP2000/MMT		52	53			4
POP4000/MMT		92	70			8
			POP2000/MMT-Iron Oxide			
method a	50/50	14	15	71	none	
method b	50/50	14	13	75		
	83/17	18	18	66	0.36	
			POP4000/MMT-Iron Oxide			
method B	50/50		28	60	12.6	2
	83/17	50[d]	51	27	3.4	4

[a] Organic fraction in organoclays analyzed by TGA. [b] The reduction of organic weight fraction (by TGA) before and after the iron-ion addition. [c] The weight ratio of absorbed crude oil by the organoclay samples. [d] Based on TEM.

the multilayered spacing in creating an interlayer space volume more than five times that of the pristine clay. In particular, the uses of hydrophobic POP-amine-salts of 2000 and 4000 g/mol molecular weight, expands the silicate *d*-spacing from 1.2 to 5.2 and 9.2 nm, respectively (Table 1). More importantly, the POP modification altered the properties of the clay from hydrophilic to hydrophobic (40). The POP-modified organoclays are hydrophobic and dispersible in water only at low temperature because of the presence of temperature-dependent hydrogen bond interactions. The POP/MMT exhibited an inverse-temperature dispersion property or a "lower critical aggregation temperature" (LCAT) in the range of 4−30 °C. In other words, the material can only be dispersed at a temperature lower than LCAT, a behavior similar to "lower critical solution temperature" (LCST) for the common nonionic surfactants and some PEG-segmented copolymers. The water-dispersing ability is weakened because of the disruption of hydrogen bonds with water molecules above the critical temperature. The low-temperature dispersion behavior requires the synthesis of iron-oxide particles to be performed at 4 °C. At such low temperatures, the clays were less aggregated and finely dispersed with the primary structure of the multilayered space accessible for iron-oxide formation.

pH Requirement for the In situ Fe^{2+}/Fe^{3+} Coprecipitation in the Presence of POP/MMT. Because the structures of the organoclays involved an ionic complex between the POP-amine-salts and silicate counterions, the POP species in the MMT confinement is sensitive to the environmental pH. During the generation of FeNPs in the layered structure, a suitable pH environment is crucial for maintaining the POP/MMT complex. In method A, without adding HCl for pH adjustment, the process failed to produce ferromagnetic iron oxides while the silicate *d* spacing shrunk from 5.2 to 1.8 nm (Table 1). In method B, by dispersing the organoclay in deionized water at 4 °C and then adding HCl to adjust the pH to 2, the desired nanohybrid of POP2000/MMT-FeNP with 17 wt % of FeNPs in the composition was produced. The method involving low temperature and controlled low pH values was successfully developed for incorporating various amounts of FeNPs in the nanostructures from the Fe^{2+}/Fe^{3+} coprecipitation.

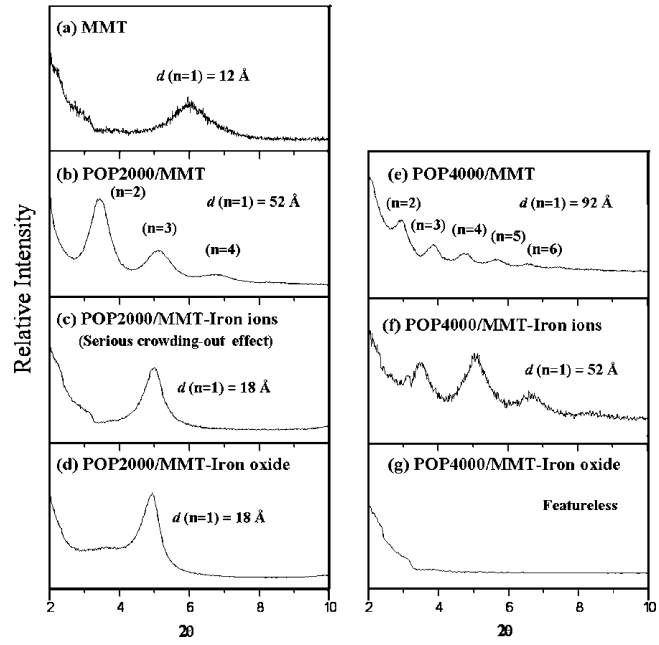

FIGURE 1. X-ray diffraction patterns of organoclay-iron oxide (83/17 by weight ratio). (a) MMT, (b) POP2000/MMT, (c) POP2000/MMT with Fe^{2+}/Fe^{3+}, (d) POP2000/MMT-iron oxide, (e) POP4000/MMT, (f) POP4000/MMT with Fe^{2+}/Fe^{3+}, and (g) POP4000/MMT-iron oxide.

Crowding-out Effect or the Replacement of POP by Fe^{2+}/Fe^{3+} in Clay Confinement. It is noted that the existence of POP in the gallery may initially attract Fe^{2+}/Fe^{3+} in high local concentration. However, the ion diffusion and accumulation could cause the replacement of organic salts in the galleries and result in a collapse of the silicate layer spacing before the FeNPs formation. With the XRD analyses shown in Figure 1, it was observed that the addition of Fe^{2+}/Fe^{3+} caused the *d* spacing to shrink from 5.2 to 1.8 nm for the POP2000 and from 9.2 to 5.2 nm for the POP4000 composites. The release of POP-salts from the MMT galleries is defined as a crowding-out effect or the POP replacement by the iron ion exchanging reaction. Although the final POP/MMT-iron oxide maintained some of magnetism, the POP was largely reduced from the originally high composition of 53 wt % to only 18 wt % for the POP2000 and 70 to 51 wt % for POP4000 composites, as shown in Table 1. For the XRD analyses, there was observed a featureless pattern for POP4000/MMT-iron oxide, perhaps due to the reasons of MMT layer randomization. It was found that the use of the POP4000/MMT precursor could minimize the silicate shrinking and maintain most of the organic fraction during the formation of iron oxides. As a result, the POP4000/MMT precursor was a better "container" for accommodating the formation of FeNPs within the layered structure.

Characterization of Magnetic Property. In the control experiment without the clay, the coprecipitation of Fe^{2+}/Fe^{3+} salts at the specific 1:2 ratio generated the iron-

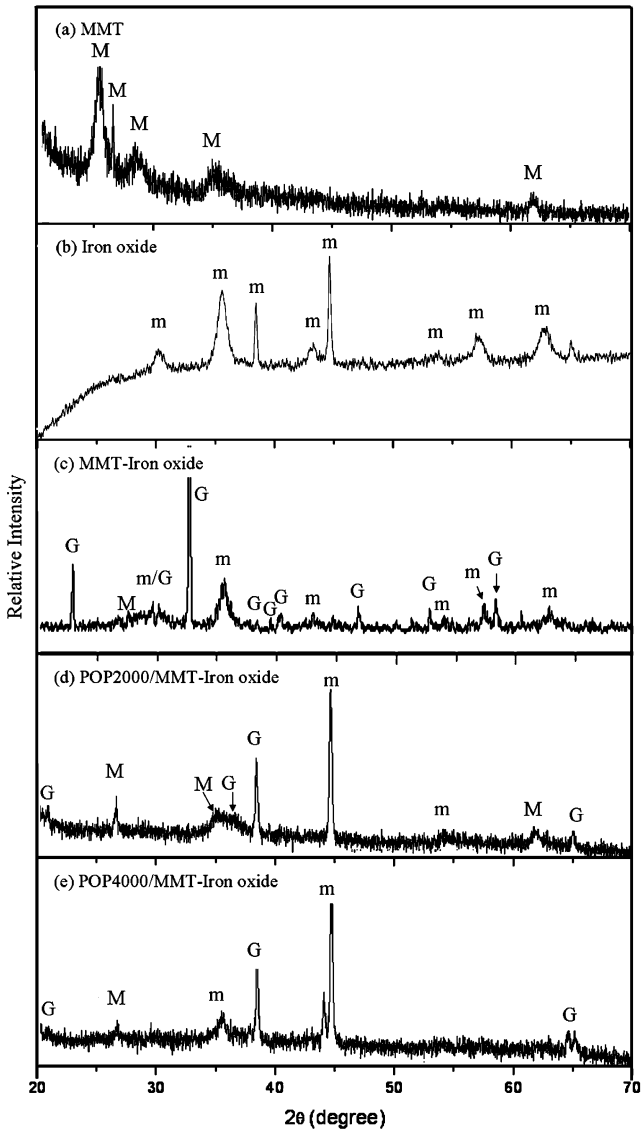

FIGURE 2. X-ray diffraction patterns of organoclay-iron oxide (83/17 by weight ratio): (a) MMT, (b) iron oxide, (c) MMT-iron oxide, (d) POP2000/MMT-iron oxide, and (e) POP4000/MMT-iron oxide (M, MMT; m, maghemite; and G, goethite.)

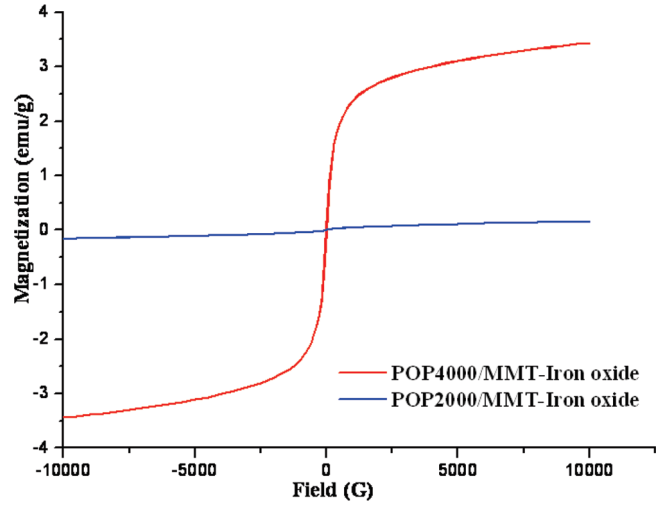

FIGURE 3. Magnetization of POP2000 and POP4000 derived nanohybrids at the composition of 83/17 weight ratio (organoclay-iron oxide).

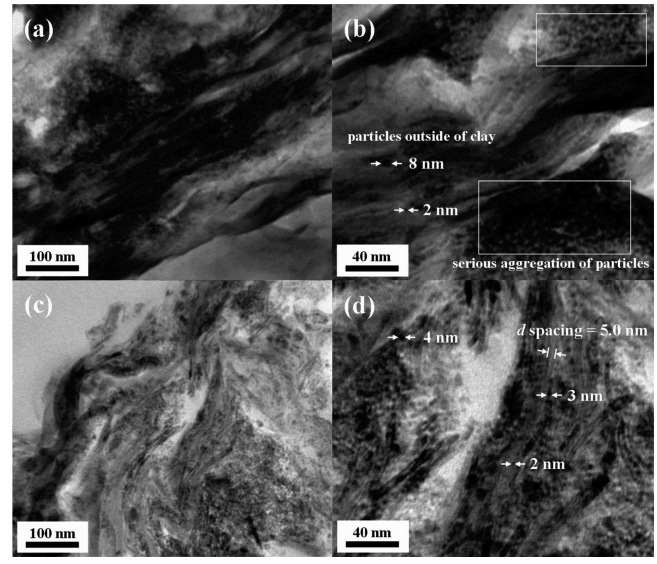

FIGURE 4. TEM micrographs of organoclay-iron oxide (83/17 by weight ratio): (a)(b) POP2000/MMT-iron oxide showing the clusters of particle aggregates (particle size = 2−8 nm), and (c)(d) POP4000/MMT-iron oxide showing the clay platelets in parallel (at average *d* spacing of 5 nm) and iron oxide particles in the interlayer (particle size = 2−4 nm).

oxide particles (Figure 2) with the characteristic peaks for the magnetite of γ-Fe_2O_3 (maghemite). With the presence of MMT or organoclays, the involved ion exchange between the metal ions and POP salts causes a deviation from the specific 1:2 ratio that is required for the formation of magnetic particles, perhaps through silicate surface interference. By comparing the MMT reference peaks, two species of iron oxide were characterized for γ-Fe_2O_3 and FeOOH (goethite) (17). The species of magnetic γ-Fe_2O_3 in POP4000 appeared to be richer than that in POP2000 nanohybrid. The appearance of darker color for the γ-Fe_2O_3 presence was compared for the two samples (see the Supporting Information, Figure S1).

Although both POP4000/MMT- and POP2000/MMT-FeNP nanohybrids exhibited similar XRD peaks, the former with a composition of 83/17 (organoclay/FeNP weight ratio), demonstrated a stronger magnetism (Figure 3) due to the presence of γ-Fe_2O_3. By comparison, the nanohybrid with an increased composition of iron oxide at 50/50 ratio had an enhanced magnetism with a hysteresis loop, while decreased in toluene solvating ability. Consequently, the 50/50 hybrid exhibited a lowering of crude oil adsorption ability from 4 times the oil weight to only 2 (Table 1).

Morphologies of the Nanohybrids under Transmission Electronic Microscopy. The morphologies of the nanohybrids at 83/17 weight ratio or 17 wt % iron-oxide in the composite were examined by TEM. Possible interference of the electron beam caused by the iron-oxide ferromagnetism may explain the blurry image. In images a and b in Figure 4, the POP2000/MMT-FeNP was shown to have iron-oxide particles in the size of 2−8 nm diameter, aggregated into clusters and located outsides the clay interlayer galleries. By comparison, the particles with a diameter of 2−4 nm are embedded in the interlayer structure of

Scheme 1. Conceptual Illustration of the Generation of Iron-Oxide Particles from Fe^{2+}/Fe^{3+} Coprecipitation and Their Association with the Layered Silicate Structure

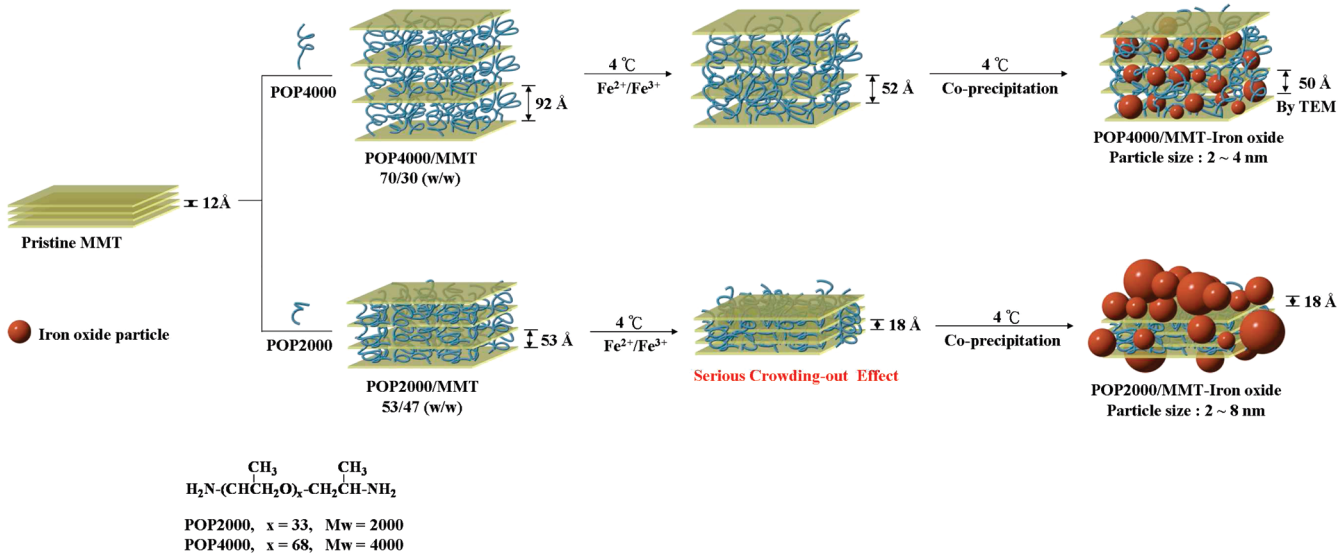

POP4000/MMT (Figure 4c, d), where the parallel lines of platelet side view are observed and estimated to have ca. 5.0 nm basal spacing for a local area. The observation provided evidence of the FeNP existence in the silicate layered structure.

Performances of POP/MMT-FeNP Nanohybrids. A conceptual diagram (Scheme 1) illustrates the process of POP intercalation, in situ Fe^{2+}/Fe^{3+} coprecipitation of FeNPs in the clay layered structure. Two different modes of the particle association with MMT are largely decided by the POP2000 or POP4000 intercalation with different *d* spacing. In the case of POP2000/MMT, the silicate shrunk from 5.2 to 1.8 nm during the Fe^{2+}/Fe^{3+} addition. A crowding-out effect occurred due to the ionic exchange reaction with the POP organics. As a result, the generated iron-oxide particles seriously aggregated and were adsorbed onto the clay surface rather than an embedded in the gallery. With the POP4000/MMT, the larger *d* spacing correlates to higher organic content and a diminished crowding-out effect throughout the process. The nanohybrid was found to have a final *d* spacing (5.0 nm) that provided space for the FeNP embedment. Two nanohybrids demonstrated similar sets of XRD diffraction peaks as shown in Figure 2. However, the analysis indicated that the FeNPs in POP2000/MMT had a rather weak magnetism in comparison to that of the POP4000/MMT-FeNP (Figure 3), which was further shown to be superparamagnetic because of the zero coercive force. Overall, the initial existence of POP4000 in the precursor clay is crucial to avoid the crowding-out effect or the replacement of POP salts and consequently maintain more room for accommodating FeNPs. The formation of FeNPs in the silicate-layered confinement is less aggregated and better dispersed through the POP association.

Simulation of Remedying Pollutant or Spilt Oil. With dual components of POP and magnetic iron-oxide particles in the silicates, the nanohybrids are suitable for adsorbing hydrophobic organics. As a demonstration shown in Figure 5 and Movie S1 of the Supporting Information, the high-organic-fraction composite of POP4000/MMT-FeNP (51/32/17 by weight) enabled the adsorption of petroleum crude oil from the water slurry. A control experimental is used to confirm the maximum adsorption capacity of crude oil on the pristine organoclay. In the case of POP4000/MMT, there is an 8-fold increase in weight-based capacity of the crude oil. A decrease of the adsorption capacity (2 or 4 folds) was observed when introducing iron-oxide particles in the composite. However, the nanohybrids gained magnetism while remaining the hydrophobic affinity. Hence, the exemplified nanohybrid demonstrated an increased ability to adsorb crude oil by 4-fold based on weight, an ability to agglomerate the adsorbed oil into lumps and is movable under an applied magnetic field. The prepared nanohybrid with the functions of oil adsorption and collectable under magnetic field is advantageous over the conventional absorbents for waste product (54).

CONCLUSION

Magnetic FeNPs were successfully synthesized from in situ particle embedment within the layered MMT structure that was previously modified by hydrophobic POP-amine-salts. By main-

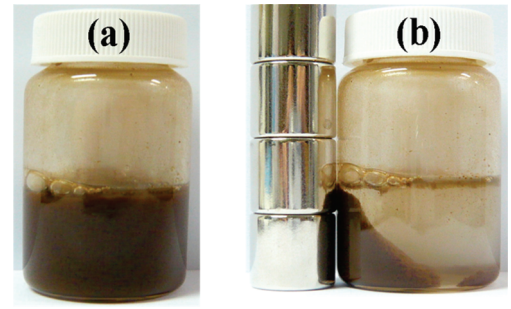

FIGURE 5. Photographs of the dispersions of POP4000/MMT-iron oxide (51/32/17 by weight ratio): (a) adsorbtion of four times crude oil by weight, and (b) application of a magnet bar to attract the lumps of aggregated crude oil to one side of the vial.

taining a low temperature (4 °C) and pH allowed the POP/MMT dispersion in water without serious aggregation during the Fe^{2+}/Fe^{3+} coprecipitation. The POP4000-intercalated MMT organoclay with the composition of 70 wt % organics and wide basal spacing of 9.2 nm was more suitable for the FeNP embedment than the POP2000/MMT. An unwanted "crowding-out effect" may shrink the clay basal spacing to 1.8 nm and disallow particle incorporation. With POP4000, the modified clay accommodated the FeNPs (17 wt % at 2−4 nm diameter) along with 51 % POP in the layered gallery of 5.0 nm basal spacing. With the combined hydrophobic and superparamagnetic properties, the synthesized nanohybrid demonstrated the ability to adsorb crude oil from water four times the weight, form agglomerated oil lumps and be maneuverable under a simple magnetic field. By varying the POP/FeNP composition in the silicate multilayered structure, the nanohybrids are able to adsorb hydrophobic materials and then be efficiently removed using simple magnetic fields making it ideal for mechanical environment-cleaning applications involving crude oil or possibly other hydrophobic pollutants.

Supporting Information Available: Color comparison and magnetism of POP2000/MMT-iron oxide, POP4000/MMT-iron oxide composites, and iron oxide (PDF); a video showing an efficient removal of the nanohybrid with adsorbed oil by a magnetic field within 30 s (MPG). This material is available free of charge via the Internet at http://pubs.acs.org.

Acknowledgment. This work was financially supported by the National Science Council (NSC) of Taiwan and partially by Ministry of Economic Affairs, Taiwan.

REFERENCES AND NOTES

(1) Hu, S. H.; Liu, T. Y.; Huang, H. Y.; Liu, D. M.; Chen, S. Y. *Langmuir* **2008**, *24*, 239–244.
(2) Cheng, F. Y.; Su, C. H.; Yang, Y. S.; Yeh, C. S.; Tsai, C. Y.; Wu, C. L.; Wu, M. T.; Shieh, D. B. *Biomaterials* **2005**, *26*, 729–738.
(3) Lin, C. L.; Lee, C. F.; Chiu, W. Y. *J. Colloid Interface Sci.* **2005**, *291*, 411–420.
(4) Enzel, P.; Adelman, N. B.; Beckman, K. J.; Campbell, D. J.; Ellis, A. B.; Lisensky, G. C. *J. Chem. Educ.* **1999**, *76*, 943–948.
(5) Lin, Y. J.; Wang, L.; Lin, J. G.; Huang, Y. Y.; Chiu, W. Y. *Synth. Met.* **2003**, *135−136*, 769–770.
(6) Liu, Z. L.; Wang, X.; Yao, K. L.; Du, G. H.; Lu, Q. H.; Ding, Z. H.; Tao, J.; Ning, Q.; Luo, X. P.; Tian, D. Y.; Xi, D. *J. Mater. Sci.* **2004**, *39*, 2633–2636.
(7) Franger, S.; Berthet, P.; Berthon, J. *J. Solid State Electron.* **2004**, *8*, 218–223.
(8) Yu, W. W.; Falkner, J. C.; Yavuz, C. T.; Colvin, V. L. *Chem. Commun.* **2004**, *20*, 2306–2307.
(9) Wu, M.; Xiong, Y.; Jia, Y.; Niu, H.; Qi, H.; Ye, J.; Chen, Q. *Chem. Phys. Lett.* **2005**, *401*, 374–379.
(10) Gangas, N. H. J.; Wonterghem, J. V.; Morup, S.; Koch, C. J. W. *J. Phys. C: Solid State Phys.* **1985**, *18*, L1011–L1015.
(11) Doff, D. H.; Gangas, N. H. J.; Allan, J. E. M.; Coey, J. M. D. *Clay Minerals* **1988**, *23*, 367–377.
(12) Miyoshi, H.; Yoneyama, H. *J. Chem. Soc., Faraday Trans. 1* **1989**, *85*, 1873–1880.
(13) Mori, H.; Miyoshi, H.; Takeda, K.; Yoneyama, H.; Fujita, H.; Iwata, Y.; Otsuka, Y.; Murata, Y. *J. Mater. Sci.* **1992**, *27*, 3197–3199.
(14) Heylen, I.; Vanhoof, C.; Vansant, E. F. *Microporous Mater.* **1995**, *5*, 53–60.
(15) Bourlinos, A. B.; Karakassides, M. A.; Simopoulos, A.; Petridis, D. *Chem. Mater.* **2000**, *12*, 2640–2645.
(16) Oliveiraa, L. C. A.; Petkowiczb, D. I.; Smaniottob, A.; Pergherb, S. B.C. *Water Res.* **2004**, *38*, 3699–3704.
(17) Oliveira, L. C. A.; Rios, R. V. R. A.; Fabris, J. D.; Sapag, K.; Garg, V. K.; Lago, R. M. *Appl. Clay Sci.* **2003**, *22*, 169–177.
(18) Booker, N. A.; Keir, D.; Priestley, A. J.; Ritchie, C. B.; Sudarmana, D. L.; Woods, M. A. *Water Sci. Technol.* **1991**, *23*, 1703–1712.
(19) Orbell, J. D.; Godhino, L.; Bigger, S. W.; Nguyen, T. M.; Ngeh, L. N. *J. Chem. Educ.* **1997**, *74*, 1446–1448.
(20) Cseri, T.; Bekassy, S.; Figueras, F.; Rizner, S. *J. Mol. Catal. A: Chem.* **1995**, *98*, 101–107.
(21) Pinnavaia, T. J. *Science* **1983**, *220*, 365–371.
(22) Ajjou, A. N.; Harouna, D.; Detellier, C.; Alper, H. *J. Mol. Catal. A: Chem.* **1997**, *126*, 55–60.
(23) Celis, R.; Hermosin, M. C.; Carrizosa, M. J.; Cornejo, J. *J. Agric. Food Chem.* **2002**, *50*, 2324–2330.
(24) Rawajfih, Z.; Nsour, N. *J. Colloid Interface Sci.* **2006**, *298*, 39–49.
(25) Kiraly, Z.; Veisz, B.; Mastalir, A.; Kofarago, G. *Langmuir* **2001**, *17*, 5381–5387.
(26) Giannelis, E. P. *Adv. Mater.* **1996**, *8*, 29–35.
(27) Alexandre, M.; Dubois, P. *Mater. Sci. Eng.* **2000**, *28*, 1–63.
(28) Ray, S. S.; Okamoto, M. *Prog. Polym. Sci.* **2003**, *28*, 1539–1641.
(29) Theng, B. K. G. *The Chemistry of Clay−Organic Reactions*, 2nd ed.; John Wiley & Sons: New York, 1974.
(30) Olphen, H. V.; Hsu, P. H. *An Introduction to Clay Colloid Chemistry*, 2nd ed.; John Wiley & Sons: New York, 1978.
(31) Theng, B. K. G. *Formation and Properties of Clay−Polymer Complexes*; Elsevier: New York, 1979.
(32) Usuki, A.; Hasegawa, N.; Kadoura, H.; Okamoto, T. *Nano Lett.* **2001**, *1*, 271–272.
(33) Sparks, D. L. *Environmental Soil Chemistry*; John Wiley & Sons, New York, 2003.
(34) Wang, H.; Zhao, T.; Zhi, L.; Yan, Y.; Yu, Y. *Macromol. Rapid Commun.* **2002**, *23*, 44–48.
(35) Okada, A.; Usuki, A. *Mater. Sci. Eng., C* **1995**, *3*, 109–115.
(36) Okada, A.; Usuki, A. *Macromol. Mater. Eng.* **2006**, *291*, 1449–1476.
(37) Triantafillidis, C. S.; LeBaron, P. C.; Pinnavaia, T. J. *Chem. Mater.* **2002**, *14*, 4088–4095.
(38) Muzny, C. D.; Butler, B. D.; Hanley, H. J. M.; Tsvetkov, F.; Peiffer, D. G. *Mater. Lett.* **1996**, *28*, 379–384.
(39) Lin, J. J.; Cheng, I. J.; Wang, R.; Lee, R. J. *Macromolecules* **2001**, *34*, 8832–8834.
(40) Lin, J. J.; Cheng, I. J.; Chou, C. C. *Macromol. Rapid Commun.* **2003**, *24*, 492–495.
(41) Chou, C. C.; Chang, Y. C.; Chiang, M. L.; Lin, J. J. *Macromolecules* **2004**, *37*, 473–477.
(42) Lin, J. J.; Wei, J. C.; Tsai, W. C. *J. Phys. Chem. B* **2007**, *111*, 10275–10280.
(43) Lin, J. J.; Wei, J. C.; Juang, T. Y.; Tsai, W. C. *Langmuir* **2007**, *23*, 1995–1999.
(44) Usuki, A.; Kawasumi, M.; Okada, A.; Kurauchi, T. *J. Mater. Res.* **1993**, *8*, 1174–1178.
(45) Chou, C. C.; Shieu, F. S.; Lin, J. J. *Macromolecules* **2003**, *36*, 2187–2189.
(46) Vaia, R. A.; Teukolsky, R. K.; Giannelis, E. P. *Chem. Mater.* **1994**, *6*, 1017–1022.
(47) Zhu, Z. k.; Yin, J.; Wang, X. Y.; Qi, Z. E. *Polymer* **1999**, *40*, 4407–4414.
(48) Fu, X.; Qutubuddin, S. *Mater. Lett.* **2000**, *42*, 12–15.
(49) Fu, X.; Qutubuddin, S. *Polymer* **2001**, *42*, 807–813.
(50) Zeng, C.; Lee, L. J. *Macromolecules* **2001**, *34*, 4098–4103.
(51) Hotta, S.; Paul, D. R. *Polymer* **2004**, *45*, 7639–7654.
(52) Maiti, M.; Bandyopadhyay, A.; Bhowmick, A. K. *J. Appl. Polym. Sci.* **2006**, *99*, 1645–1656.
(53) Mahadevaiah, N.; Venkataramani, B.; JaiPrakash, B. S. *Chem. Mater.* **2007**, *19*, 4606–4612.
(54) Gupta, V. K.; Suhas, *J. Environ. Manage.* **2009**, *90*, 2313–2342.

AM100019T